In Situ Self-Folding Assembly of a Multi-Walled Hydrogel Tube for Uniaxial Sustained Molecular Release

*Kwanghyun Baek, Jae Hyun Jeong, Artem Shkumatov, Rashid Bashir, and Hyunjoon Kong**

For the last several decades, hydrogels have been increasingly used to control the spatiotemporal distributions of various diagnostic and therapeutic bioactive molecules within tissues of interest through local and sustained molecular release.[1,2] To attain this goal, extensive efforts have been made to control gel properties (i.e., degradation rates, interaction with bioactive molecules, etc) mainly by chemically modifying gel-forming polymers; however, these approaches often encounter several challenges including maintaining the structural integrity of the gels, the denaturation of macromolecules, and a limited transport of macromolecules into target tissue.[3,4] To resolve these challenges, this study presents a simple, but unprecedented method to control the direction and kinetics of molecular release using a multi-walled poly(ethylene glycol) diacrylate (PEGDA) hydrogel tube formed by self-folding of a bi-layered gel patch. This self-folding property was attained by forming double-layered hydrogel patches with significantly different expansion ratios and elastic moduli. The diameter of the gel tubes could be predicted by an equation used to estimate the curvature of a bimorph beam. The resulting gel tubes exhibited a sustained release of molecules solely through its internal wall. Multi-walled gel tubes were further used as a carrier of vascular endothelial growth factor (VEGF) to demonstrate that the unidirectional, sustained VEGF release significantly increased both the density and diameters of blood vessels around the implant site, compared to unfolded hydrogel patches. This multi-walled gel tube will greatly serve to improve the efficacy of various diagnostic and therapeutic molecules.

Prof. H. Kong
Department of Chemical
and Biomolecular Engineering
Micro and Nanotechnology Laboratory
Institute of Genomic Biology
University of Illinois at Urbana-Champaign
Urbana, Illinois 61801, USA
E-mail: hjkong06@illinois.edu

K. Baek
Department of Materials Science and Engineering
University of Illinois at Urbana-Champaign
Urbana, Illinois 61801, USA

Dr. J. H. Jeong
Department of Chemical and Biomolecular Engineering
University of Illinois at Urbana-Champaign
Urbana, Illinois 61801, USA

A. Shkumatov
Department of Pathobiology
University of Illinois at Urbana-Champaign
Urbana, Illinois 61801, USA

Prof. R. Bashir
Department of Electrical and Computer Engineering
Department of Bioengineering
Micro and Nano Technology Lab
Institute of Genomic Biology
University of Illinois at Urbana-Champaign
Urbana, Illinois 61801, USA

DOI: 10.1002/adma.201300951

Prior approaches to control the release of molecules from hydrogels largely focused on chemically coupling molecules of interests to the gel-forming polymers using hydrolytically or enzymatically labile units.[5] Alternatively, efforts have been made to chemically modify gel-forming polymers with oligopeptides or proteins that can physically associate with molecules of interests.[6] These approaches have demonstrated several impressive results; however, multiple chemical modifications and purification steps often increase material costs, and also readily denature the encapsulated compounds.[4] Additionally, the degradation process typically reduces a gel's rigidity and resistance to fracture, thus leading to an undesirable structural disintegration of the gel at an implantation site.[7] The degradation may also expedite denaturation of compounds due to pH changes and the formation of reactive species.[8] Separately, the interface formed between a gel implant and the target tissue acts as a physical barrier that limits molecular diffusion into the target tissue.[9] Microfabrication techniques have been used to introduce microchannels in a gel's structure, in order to facilitate the release of molecules into tissues; however, there is still a need to develop simpler processes that are compatible with a wide array of cross-linking mechanisms used to fabricate and assemble hydrogel structures.[10,11]

We hypothesized that a gel patch consisting of two layers with significantly different stiffness and capacities to uptake water would self-fold into a multi-walled gel tube when exposed to aqueous media. The resulting gel tube would display a sustained molecular release exclusively from the internal wall of the multiwall system. This hypothesis was examined by assembling a bi-layered gel patch, in which each layer consisted of PEGDA with different molecular weights (MW) and concentrations. The material's ability to control the direction and rate of molecular release was examined by encapsulating a small colorant or bovine serum albumin (BSA) into an inner hydrogel layer of the gel tube. Finally, a bi-layered PEGDA hydrogel encapsulating VEGF was implanted on a chicken chorioallantoic membrane (CAM) to evaluate the in situ gel tube formation and neovascularization.

The self-folding bi-layered hydrogel patch was assembled by first preparing a thin hydrogel of PEGDA with a MW of 400 g mol^{-1}, termed as PEGDA400, by exposing the pre-gel

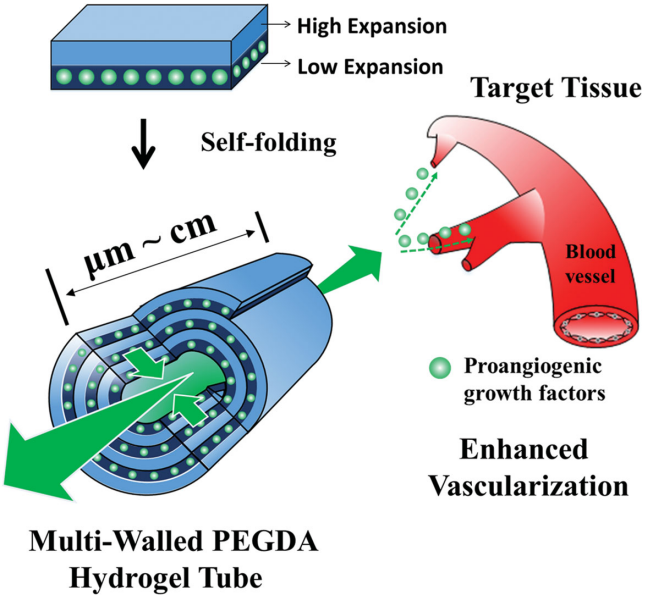

Scheme 1. Schematic depicting multi-walled PEGDA hydrogel tube that sustainably releases encapsulated growth factors in uniaxial direction and subsequently enhances neovascularization.

solution to ultraviolet (UV) light. Subsequently, another hydrogel layer was prepared over the PEGDA400 hydrogel by cross-linking the higher MW PEGDA solution (**Scheme 1**). The polymer concentration of each layer was kept constant at 20%. Each hydrogel thickness was kept constant at 200 μm. No physical separation was found between two gel layers.

The subsequent immersion of the hydrogel patches in deionized water or phosphate buffer saline (PBS) triggered self-folding into a multi-walled gel tube, exclusively for the gel patches in which the top gel layer was PEGDA with MW larger than 1000 g mol^{-1} (**Figure 1**a). According to the magnetic resonance image of the gel tube, the PEGDA400 gel layer laden with iron oxide nanoparticles was wrapped by the higher MW PEGDA gel layer. Therefore, the internal wall of the tube consisted of the PEGDA400 gel, while the external surface was the larger MW PEGDA gel layer (Figure 1b).

The geometries of the gel tubes were dependent on differences in the MW and concentrations between PEGDA gel layers. Increasing the MW of PEGDA in the top layer resulted in an exponential decrease in the elastic modulus and a linear increase of the one-dimensional expansion ratio as defined in Equation (1),

$$S = \left(\frac{Q_f}{Q_i}\right)^{\frac{1}{3}} - 1 \quad (1)$$

where Q_i and Q_f are the degrees of swelling of a hydrogel before and after incubation in aqueous media, respectively (Figure 1c, S1 and Table S1, Supporting Information). Specifically, bi-layered gel patches with 2 cm length and 2 cm width were self-folded into tubes with 2 cm length (Figure S2). The inner radius of the tube decreased from 9 to 0.7 mm by increasing the MW of the upper gel layer from 1000 to 10 000 g mol^{-1} (Figure 1a-1 & 1d). The same result was obtained with hydrogel strips with the same length but 1 mm wide. The two-layered gel strips were self-folded into tubes with 1 mm length, while the inner radius of the tube was decreased by increasing the difference in MW (Figure 1a-2 and 1d). Additionally, this decrease in the inner radius was inversely related to thickness of the tube wall (Figure 1d).

To understand the underlying mechanism, the inverse dependency between the inner radius of the gel tube and the difference of MW was fitted to a mathematical model originally developed to estimate the curvature of a heat-induced bimetallic strip (Equation (2)),

$$r = \frac{h}{12 \in}\left(\frac{E_1}{E_2} + 14 + \frac{E_2}{E_1}\right) \quad (2)$$

where r is the inner radius of the gel tube, E_1 and E_2 are the elastic moduli of the bottom PEGDA400 gel layer and the top PEGDA gel layer, respectively, h is the thickness of each gel layer, and ε is the difference in the expansion ratio between two gel layers (ΔS).[12] This mathematical model therefore suggests that the larger ε leads to a decrease of r, coupled with the E_1/E_2. Incorporating measured E and ε into Equation (2) resulted in estimations of r values which decrease by increasing the difference in MW of PEGDA between the two layers, similar to the experimental results. More interestingly, these calculated r values agreed with the experimental values (Figure 1d). This result, therefore, suggests that the inverse relationship between the r value and the difference in MW of PEGDA is due to changes in ε and E_1/E_2.

The inner radius and thickness of the gel tube was further modulated with the polymer concentration of the PEGDA400 gel layer (Figure S3). According to measurements of elastic moduli and expansion ratios of the gels, decreasing the concentration of PEGDA from 30 to 10% (w/w) significantly reduced the elastic moduli from 1.3 to 0.03 MPa and increased the degree of swelling from 5 to 10; however, there was a minimal change in the expansion ratio (Figure 1e and S4, Table S1). Decreasing the polymer concentration of the PEGDA400 gel layer from 20 to 10% (w/w) decreased the inner radius from 1.0 to 0.8 mm and also increased the wall thickness from 0.9 to 1.1 mm (Figure 1f). Again, this decrease in the inner radius of the gel was in agreement with the mathematical model noted in Equation (2). These results show that the inverse relationship between the inner radius of the gel tube and polymer concentration of the gel is mainly related to changes in E_1/E_2.

The inner radii of self-folded gel tubes were further related to the differences of cross-linking density between two gel layers (N), calculated by Equation (S2) in the Supporting Information (Table S1). The inner radius of the gel tube was exponentially decreased by increasing difference of N, which was tuned by altering difference of MW of PEGDAs used to prepare the bi-layered hydrogel patch (Figure S5a). In contrast, the inner radius of the gel tube was linearly increased with difference of N, which was tailored by altering concentration of PEGDA400 pre-gel solution in the bi-layered gel patch consisting of PEGDA400 and PEGDA3400 gel layer (Figure S5b). Separately, cross-linking density of two gel layers was tailored to be similar to each other using PEGDA400 and PEGDA10000, in order to examine whether the gel still self-folds at zero-difference of N between two gel layers. The gel could still self-fold due to the

Adv. Mater. **2013**,
DOI: 10.1002/adma.201300951

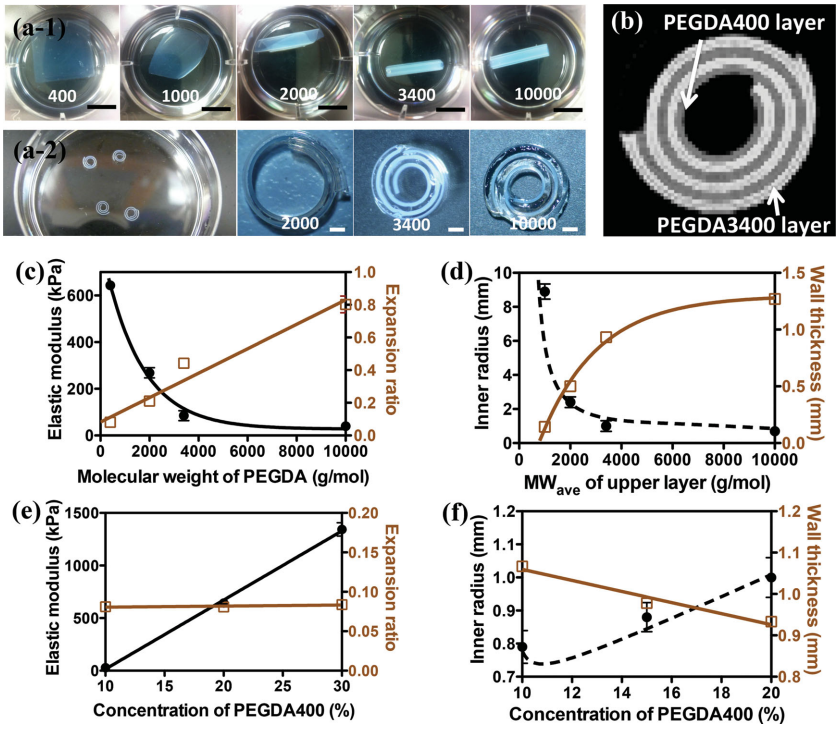

Figure 1. Effects of different molecular weights (MW) and concentrations of PEGDA hydrogels on the self-folding of the bi-layered PEGDA gel. (a) Optical images of self-folded hydrogel tubes. Images in (a-1) are lateral views of tubes with 20 mm length and images in (a-2) are cross-sectional views of tubes with 1 mm length. The numbers in each image represent the MWs of PEGDA used to prepare the top-layer in the bi-layered gel patch. Polymer concentrations of the bottom PEGDA400 gel layers and the top high MW PEGDA gel layers were kept constant at 20% (w/w). All scale bars represent 1 cm. (b) A magnetic resonance image of the cross-sectional view of the multi-walled PEGDA gel tube, in which iron oxide nanoparticles are loaded into the PEGDA400 gel layer. (c) The elastic moduli (●) and expansion ratios (□) of the hydrogels prepared with PEGDA of different MWs. (d) The dependencies of the inner radii (●) and wall thicknesses (□) of the gel tubes on the difference in the MW of PEGDA gel layers. Data points represent average values of four different experiments per condition, and a dashed curve represents the simulated result. (e) Elastic moduli (●) and expansion ratios (□) dependency on the PEGDA400 concentration in the bi-layered gel patch. (f) Dependencies of the inner radii (●) and wall thicknesses (□) of the self-folded gel tube on PEGDA400 concentration of the gel layer. A dashed curve represents the simulated result. In (e) and (f), the bi-layered gel construct was constituted with the PEGDA400 gel and PEGDA3400 gel.

difference of expansion ratio between two gel layers (Table S2 and Figure S6). Taken together, we interpret that the self-folding mechanism is not simply explained by the difference of cross-linking density between two gel layers.

The multi-walled PEGDA hydrogel tubes were further used as a molecular releasing device by encapsulating bovine serum albumin (BSA) into the PEGDA400 gel layer during the cross-linking reaction. Interestingly, the resulting gel tubes more sustainably released BSA than the unfolded gel patches (**Figure 2**a). The BSA-encapsulating single-layered PEGDA400 hydrogel patches displayed a large initial burst release of BSA, followed by rapid release. Therefore, most of the BSA loaded in the gel diffused out within 5 days. In contrast, multi-walled gel tubes exhibited an 80% lower BSA burst for the first 24 hours. The release rate quantified with a first-order kinetic approximation, β in Equation (3), was also 90% lower for the multi-walled gel tube (Table S3),

$$\frac{C_{BSA}}{C_{BSA,O}} = e^{-\beta t} \quad (3)$$

where C_{BSA} is the amount of BSA remaining in the hydrogel at time t, and $C_{BSA,O}$ is the amount of BSA initially loaded in the hydrogel.[13] Similarly, VEGF was released from the self-folded gel tube more sustainably than the gel patch (Figure S7).

To further examine whether BSA is locally released from the internal wall of the tube, we estimated the concentration distribution of BSA discharged from the unfolded PEGDA hydrogel patches and the multi-walled gel tubes, using a diffusion-based finite element method (FEM) (Figure 2a,b-1). Diffusion coefficients for the BSA release in simulations were calculated from the experimental values displayed in Figure 2a, using Equation (4),

$$\frac{M_t}{M_\infty} = 4\left(\frac{Dt}{\pi L^2}\right)^{\frac{1}{2}} \quad (4)$$

where M_t and M_∞ are the cumulative amounts of drug released at time t and at an infinite time, respectively; D is the diffusion coefficient of the drug within the system; and L is thickness of the hydrogel patch or tube wall.[13] The released BSA amount estimated by the FEM-based simulation agreed with the experimentally measured values.This simulation also discloses a continued increase in the local BSA concentration within the multi-walled gel tube, independent of the tube length (Figure 2b,c).

Furthermore, simulations were conducted to examine the diffusion of BSA and VEGF released from the multi-walled gel tubes into tissues for drug release applications. In the simulation, the self-folded gel tube with length of 1 mm was vertically implanted on tissue with the hydrogel ring and the strip as controls. The membrane implanted with the self-folded gel tube exhibited a more sustained increase of the amount of BSA and VEGF than three other controls (Figure 2c and Figure S8). The local increase of protein concentration was attributed to the release of proteins from the inner layer of the gel tube. In contrast, other three control gel implants did not result in local increase of proteins in close proximity of gel implants.

To validate these simulation results, we incorporated a colorant, 2,2′-Bis(2,3-dihydro-3-oxoindolyliden), into the PEGDA400 gel for monitoring the direction of molecule release within a short time period. Very interestingly, the colorant loaded into the multi-walled hydrogel tube with 2 cm length was released exclusively through two open ends of the gel tube (Figure 2b-2). No significant circumferential diffusion of the BSA was observed. In the same manner, the gel tube with 1 mm length, which was vertically placed on a glass surface,

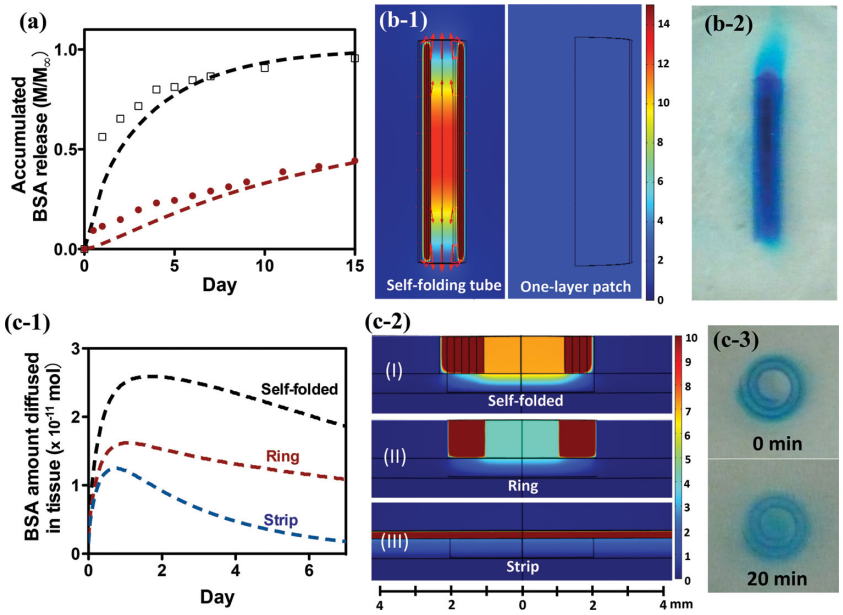

Figure 2. Experimental and computational analysis on rate and direction of molecular release from the unfolded gel patch and the multi-walled hydrogel tube. (a) The BSA release profile of the PEGDA400 gel patch (□) and multi-walled gel tube (●) consisting of a PEGDA400 gel layer and PEGDA3400 gel layer. Data points represent the average values of the experimentally measured BSA amount and dashed curves represent the simulated result. (b) Numerical and experimental analysis of the BSA release from the gel tube. (b-1) Simulated concentrations of BSA through multi-walled gel tubes with 1 mm radii and 20 mm length (left image) and PEGDA 400 gel patches with 20 mm width and 20 mm length (right image) after incubation for 10 days. Arrows represent the direction of BSA release through the hollow core of the tube. (b-2) An optical image to exhibit unidirectional release of a colorant, 2,2′-Bis(2,3-dihydro-3-oxoindolyliden), through two open ends of the gel tube. (c) Numerical and experimental analysis of BSA distribution released into a tissue membrane, following the release from the gel tube. (c-1) Numerical analysis of BSA concentrations in local tissue membrane implanted with the self-folded gel tube, the gel ring and the gel strip. The analyzed area of membrane is within horizontal radius of 2 mm and vertical distance of 500 μm from the center of gel implant. (c-2) Simulated concentration distribution of BSA released into tissues implanted with the self-folded hydrogel tube with 1 mm inner radius and 1 mm length (I), the hydrogel ring with 2 mm outer radius and 1 mm inner radius (II) and the hydrogel strip with 1 mm width and 20 mm length (III) (lower image), after five days of implantation. The gel tube was vertically implanted. (c-3) Optical images of the colorant released into the hollow core of the gel tube. The units for the simulation scale bars are mmol m^{-3}.

also exhibited diffusion of the colorant through the internal wall (Figure 2c-3).

Finally, the gel tube encapsulating VEGF was implanted on a chicken chorioallantoic membrane (CAM) to test whether the local sustained VEGF release stimulates vascularization at an implantation site. In this experiment, the bi-layered PEGDA gel encapsulating VEGF in the PEGDA400 gel layer was assembled into a strip with 2 cm length and 1 mm width. Then, the bi-layered hydrogel strip was implanted on the CAM. The strip self-folded into a tube with 1.3 mm inner radius, 1 mm height, and 700 μm wall thickness within 10 minutes (**Figure 3**a). Within 7 days, the VEGF-encapsulated self-folded hydrogel tube significantly stimulated blood vessel growth around the implant, as compared to other controls, including the VEGF-encapsulating hydrogel ring with 2.2 mm outer radius and 1.3 mm inner radius, VEGF-encapsulated hydrogel disk with 2.2 mm radius and the VEGF-encapsulating PEGDA400 hydrogel strip. The VEGF amount loaded in each gel implant was kept constant at 60 ng, in order to examine effects of gel geometry on vascularization at the same VEGF dosage. According to our previous studies, the VEGF dosage was large enough to stimulate vascularization in CAM, when VEGF was released from a hydrogel modified to degrade hydrolytically.[14]

According to histological cross-sections of the tissues, the density of mature blood vessels positively stained by an antibody to α-smooth muscle actin was 1.5-fold larger for the VEGF-releasing multi-walled gel tubes than hydrogel rings, and 2-fold lager than other control conditions (Figure 3b,c). Additionally, there was a significant increase in the fraction of blood vessels with larger cross-sectional areas of 3000 μm^2 or greater in the membranes implanted with the VEGF-releasing gel tubes, compared to other conditions (Figure 3b and 3d). The PEGDA400 hydrogel rings and disks laden with VEGF resulted in limited vessel growth and even hydrogel strips showed similar vessel growth to the VEGF-free hydrogel tubes.

Overall, our results demonstrate a multi-walled PEGDA hydrogel tube formed from the self-folding of a gel patch composed of two layers with different elastic moduli and expansion ratios. The differential stress between the two gel layers likely drove the self-folding process, as demonstrated through both experimental results and mathematical modeling. We propose that this self-folding process is distinguishable from other self-folding polymeric materials, with regards to the strategy of using differential stress.[15,16] Previously reported materials were largely constituted with chemically dissimilar materials which present different degradation rates and thermal sensitivities. Additionally, this study highlights that the difference of the expansion ratios between two gel layers determines the inner radius of the self-folded gel tube more predominantly than difference in the degree of swelling.

Another highlight of this study is that the resulting multi-walled PEGDA hydrogel tube can sustainably release biomacromolecules solely through two open ends. We suggest that this feature is attained for the following reasons: (1) a decrease in the surface area, (2) the presence of the multi-walls, (3) a sealing of the external tube surface by the blank gel layer, and (4) heterogeneously loaded drugs in a bi-layer. The self-folding process reduced surface area of the gel layer by 84%. The BSA or VEGF release rate should be significantly decreased in proportional to the surface area. Additionally, the blank hydrogel layers between the PEGDA400 gel layers decrease the BSA diffusivity in the gel tube. Moreover, the blank gel layer on the external surface likely acted as an insulator to prevent circumferential molecular release, similar to the myelin sheath which insulates neural axons.[17] This simple, but refined

Adv. Mater. 2013,
DOI: 10.1002/adma.201300951

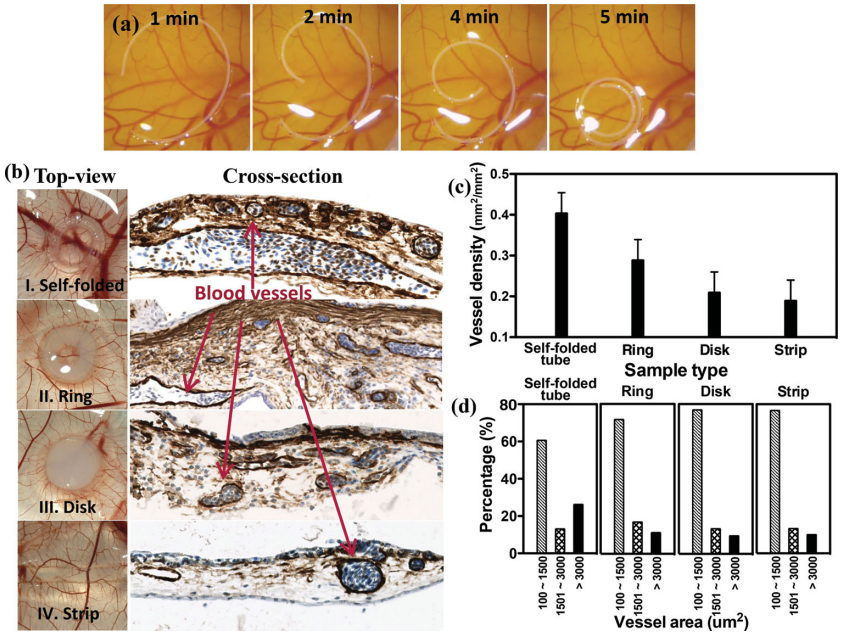

Figure 3. Enhanced vascularization with the VEGF-releasing multi-walled hydrogel tube. (a) Images of the in vivo self-folding of the bi-layered PEGDA hydrogel strips with 1 mm width and 20 mm length on CAM. (b) Optical top-view images of vascular networks and microscopic images of histological cross-sections of CAMs that were stained with a marker for α-smooth muscle actin. Samples include the CAMs implanted with multi-walled hydrogel tube with 2.2 mm outer radius, 1.3 mm inner radius and 1 mm thickness (I), the CAM implanted with a PEGDA400 gel ring with 2.2 mm outer radius, 1.3 mm inner radius and 1 mm thickness (II), the CAM implanted with a PEGDA400 gel disk with 2.2 mm radius and 1 mm thickness (III), and the CAM implanted with a PEGDA400 gel strip with 1 mm width and 20 mm length (IV). All samples were laden with VEGF of 60 ng. Concentrations of VEGF in the hydrogel tube, ring, disk and strips were 7.5, 7.5, 5.0 and 15.0 μg ml^{-1}, respectively. (c) Vascular densities of the CAM implanted with the VEGF-encapsulating gel tube, ring, disk and strip. (d) Analysis of vascular size mitigated by the VEGF-releasing devices.

controllability of the direction and kinetics of molecular release at this time has not yet been reported using any self-folding polymeric constructs.

Furthermore, this study demonstrated that the uniaxial sustained VEGF release from the internal wall of a gel tube is more advantageous to promote vascularization than the gel strip or disk. We interpret that the VEGF released within the core of the tube diffused into tissue and sustainably stimulated vascular sprouting, although its efficiency may be mitigated by the structure and rigidity of target tissue.[18] In contrast, limited vascularization in tissue implanted with the VEGF-encapsulated gel ring, disk or strip is likely due to the minimal localization of VEGF in implanted tissue. This result is in accordance with previous studies that address the role of VEGF localization in guiding capillary sprouting.[10,19]

Overall, we envision that the multi-walled hydrogel tube will be useful for the local sustained delivery of a wide array of drug molecules, and subsequently improve the quality of molecular therapies. This self-folding property can be attained by pairing a wider array of hydrogel systems which react at the interface and exhibit significantly different expansion ratios, stiffness, or both. Additionally, the self-folded shape of gels may be readily controlled by altering geometry and shape of hydrogel patch using various microfabrication technologies. Conversely, a hydrogel tube which can unfurl at an implantation site and rapidly release encapsulated molecular compounds will be also useful to improving efficacy of molecular drugs in other biological applications. Also, this construct can further be advanced by loading multiple molecular compounds used for diagnostics, imaging, and treatments in separate layers.[20] Instead of molecular compounds, the hydrogel can also be encapsulated with stem cells or islets capable or secreting multiple trophic factors, in order to release cell-secreted factors in a local and sustained manner.[21]

Experimental Section

Full experiment procedures are provided in the Supporting Information. Briefly, PEGDA with differing molecular weights were synthesized and their elastic moduli and degrees of swelling were evaluated following our previous methods.[10] To fabricate a bi-layered PEGDA patch, 20% (w/w) PEGDA400 solution including 0.1% Igacure 2959 and various materials (iron oxide nanoparticles, colorant, BSA, or VEGF) was first polymerized with UV light for 5 minutes. Then, a second hydrogel layer was prepared by photo cross-linking a 20% (w/w) solution of a different molecular weight PEGDA on top of the previously formed PEGDA400 gel. Finally, the bi-layered gel was immersed in DI water or PBS to trigger self-folding into a hydrogel tube.

The release rates of BSA and VEGF from the gel patch and tube were characterized while storing them in PBS at 37 °C. The amount of BSA and VEGF released into the media was determined by a Micro-BCA assay and anti-VEGF ELISA, respectively. The release pathways of BSA and VEGF were also estimated by a FEM-based simulation (COMSOL multiphysics 4.1). (Details in Supporting Information) Additionally, the direction of molecular release from the tube was characterized by encapsulating using a colorant, 2,2'-Bis(2,3-dihydro-3-oxoindolyliden) into the hydrogel.

The VEGF-encapsulated gel constructs were implanted onto CAM of one-week-fertilized chicken embryos, in order to examine neovascularization in vivo. After one week of implantation, the samples were excised, sectioned and stained with an antibody to α-smooth muscle actin (αSMA). The histological images of the tissue implanted with gels were further analyzed to quantify vessel densities and numbers of mature blood vessels. The tissue area within a distance of 2 mm from the center of gel implants was characterized (Figure S9).

Supporting Information

Supporting information is available from the Wiley Online Library or from the author.

Acknowledgements

This work was supported by National Science Foundation (CAREER: DMR-0847253 to H. K., STC-EBICS Grant CBET-0939511 to H. K & R. B.), US Army Telemedicine & Advanced Technology Research

Center (W81XWH-08-1-0701 to H. K. & R. B.), and The University of Illinois' Center for Advanced Study (to H. K.).

Received: March 1, 2013
Revised: May 6, 2013
Published online:

[1] E. A. Silva, D. J. Mooney, *J. Thromb. Haemost.* **2007**, *5*, 590–598.
[2] C.-C. Lin, K. S. Anseth, *Pharm. Res.* **2008**, *26*, 631–643.
[3] J. L. Drury, D. J. Mooney, *Biomaterials* **2003**, *24*, 4337–4351.
[4] S. Frokjaer, D. E. Otzen, *Nat. Rev. Drug Discov.* **2005**, *4*, 298–306.
[5] J. Zhu, *Biomaterials* **2010**, *31*, 4639–4656.
[6] D. Seliktar, *Science* **2012**, *336*, 1124–1128.
[7] S. P. Zustiak, J. B. Leach, *Biomacromolecules* **2010**, *11*, 1348–1357.
[8] W. J. Becktel, J. A. Schellman, *Biopolymers* **1987**, *26*, 1859–1877.
[9] J. A. Hubbell, *J. Control. Release* **1996**, *39*, 305–313.
[10] J. H. Jeong, V. Chan, C. Cha, P. Zorlutuna, C. Dyck, K. J. Hsia, R. Bashir, H. Kong, *Adv. Mater.* **2012**, *24*, 58-63.
[11] V. Chan, P. Zorlutuna, J. H. Jeong, H. Kong, R. Bashir, *Lab Chip* **2010**, *10*, 2062.
[12] T. W. Clyne, *Key Eng. Mater.* **1995**, *116*, 307–330.
[13] P. L. Ritger, N. A. Peppas, *J. Control. Release* **1987**, *5*, 37–42.
[14] C. Cha, R. H. Kohman, H. Kong, *Adv. Funct. Mater.* **2009**, *19*, 3056–3062.
[15] R. Fernandes, D. H. Gracias, *Adv. Drug Deliv. Rev.* **2012**, 1–11.
[16] G. Stoychev, S. Zakharchenko, S. Turcaud, J. W. C. Dunlop, L. Ionov, *ACS Nano* **2012**, *6*, 3925–3934.
[17] N. Baumann, D. Pham-Dinh, *Physiol. Rev.* **2001**, *81*, 871–927.
[18] W. Risau, *Nature* **1997**, *386*, 671–674.
[19] A. H. Zisch, M. P. Lutolf, M. Ehrbar, G. P. Raeber, S. C. Rizzi, N. Davies, H. Schmökel, D. Bezuidenhout, V. Djonov, P. Zilla, J. A. Hubbell, *FASEB J.* **2003**, *17*, 2260–2262.
[20] Y. Chen, H. Chen, D. Zeng, Y. Tian, F. Chen, J. Feng, J. Shi, *ACS Nano* **2010**, *4*, 6001–6013.
[21] J. J. Schmidt, J. Rowley, H. J. Kong, *J. Biomed. Mater. Res.* **2008**, *87A*, 1113–1122.

DOI: 10.1002/adma.201300951